Top Curr Chem (Z) (2016) 374:84
DOI 10.1007/s41061-016-0086-3

REVIEW

Applications of Accelerators and Radiation Sources in the Field of Space Research and Industry

Luigi Campajola[1] · Francesco Di Capua[1]

Received: 12 May 2016 / Accepted: 16 November 2016 / Published online: 28 November 2016

Abstract Beyond their important economic role in commercial communications, satellites in general are critical infrastructure because of the services they provide. In addition to satellites providing information which facilitates a better understanding of the space environment and improved performance of physics experiments, satellite observations are also used to actively monitor weather, geological processes, agricultural development and the evolution of natural and man-made hazards. Defence agencies depend on satellite services for communication in remote locations, as well as for reconnaissance and intelligence. Both commercial and government users rely on communication satellites to provide communication in the event of a disaster that damages ground-based communication systems, provide news, education and entertainment to remote areas and connect global businesses. The space radiation environment is an hazard to most satellite missions and can lead to extremely difficult operating conditions for all of the equipment travelling in space. Here, we first provide an overview of the main components of space radiation environment, followed by a description of the basic mechanism of the interaction of radiation with matter. This is followed by an introduction to the space radiation hardness assurance problem and the main effects of natural radiation to the microelectronics (total ionizing dose, displacement damage and the single-event effect and a description of how different effects occurring in the space can be tested in on-ground experiments by using particle accelerators and radiation sources. We also discuss standards and the recommended procedures to obtain reliable results.

This article is part of the Topical Collection "Applications of Radiation Chemistry"; edited by Margherita Venturi, Mila D'Angelantonio.

✉ Francesco Di Capua
dicapua@na.infn.it

[1] Dipartimento di Fisica "E. Pancini", Università degli Studi di Napoli Federico II, Naples, Italy

Keywords Space radiation environment · Space product assurance · Radiation hardness · Single event effect · Total ionizing dose · Displacement damage

1 Introduction

Satellites not only have a economically important impact on commercial communication systems, but they are in general critical infrastructure because of the services they provide. Satellites gather information which not only improves our understanding of the space environment and contributes to physics experiments, but is also used to actively monitor weather, geological processes, agricultural development and the evolution of natural and man-made hazards. Defence agencies depend on satellite services for communication in remote locations, reconnaissance and intelligence-gathering. Both commercial and government users rely on communication satellites to provide communication in the event of a disaster that damages ground-based communication systems, provide news, education and entertainment to remote areas and/or connect global businesses.

The space radiation environment is a hazard to most satellite missions and can lead to extremely difficult operating conditions for all of the equipment travelling in space. The performance of the various space systems, such as electronic units, sensors, power and power subsystem units, batteries, payload equipments, communication units, remote sensing instruments, data handling units, externally located units and propulsion subsystem units, is determined by the proper functioning of various electronic systems. Such systems are highly sensitive to space radiation. Radiation can lead to a degradation of the device performance or to functional failure of electronic systems. Moreover, radiation accelerates aging of the devices and materials.

The space radiation environment is complex as well as dynamic. Electrons and protons are trapped in the Earth's magnetic field. The Earth is surrounded by belts of these particles, called the Van Allen belts [1]. In addition, the magnetosphere and the Solar system are exposed to a flux of solar charged particles. Since the flux is a function of the solar activity, it may increase sharply during solar flares. Galactic cosmic rays that originate from outside of the Solar system consist of highly energetic heavy ions which can be detrimental to the proper operation of electronic systems. The characteristics of the radiation environment are strongly dependent on the date, duration and orbit of the mission.

A rigorous procedure is required to ensure that the environmental forms of radiation do not compromise the functionality and efficiency of the different devices during the expected lifetime of the mission. This procedure consists of the detailed analysis of the mission in order to evaluate the radiation dose absorbed by the various systems and of all the tests necessary to ensure that all pieces of equipment operate according to the design specifications.

2 The Space Radiation Environment

Space radiation is a combination of several components, each with quite complex dynamics, and is not distributed homogeneously in the Earth magnetosphere. The concentration and type of particles in the space environment vary significantly with altitude, angle of inclination, recent solar activity and amount of spacecraft shielding. Particles present in the Earth's space radiation environment include:

- Particles trapped by the Earth's magnetic field (mainly protons and electrons)
- Galactic cosmic rays (protons and heavy ions)
- Solar cosmic rays (protons and heavy ions).

2.1 Trapped particles

The magnetic field is generated within the Earth's core by the daily rotation of the Earth, electrical forces within the core and thermal movements. The dynamo produced in this way sustains a magnetic field which can be closely approximated to the field of a giant dipole positioned at the Earth's centre and inclined by 11.3° from the spin axis. The magnetic field generated by the Earth is called magnetosphere.

The geomagnetic field lines trap charged particles, such as electrons and protons. These trapped particles gyrate spirally around the magnetic field lines. The motion of the trapped particles forms bands of electrons and protons around the Earth, leading to the formation of at least two radiation belts that are called the Van Allen radiation belts. The inner belt [2] is populated by high-energy protons (in the 10- to 100-MeV range) at a density of about 15 protons/m^3 [3] and by electrons (energy range 50–1000 keV), and it extends from $\sim$100 km up to $\sim$6000 km in altitude. For satellites on a low Earth orbit (LEO), such as the many satellites designed to provide telephony and internet services, these trapped particles represent a hazard to the proper operation of electronic systems and to the astronauts themselves. The dependence of the proton dose rate in the inner belt as a function of altitude is shown in Table 1.

The outer belt is populated by electrons extending up to 60,000 km in altitude and with energies of up to 10 MeV. This belt is more dynamic than the inner belt and is influenced by the injection of particles from geomagnetic storms. The outer radiation belt coincides with the geostationary orbit of many communication satellites. Properties of the Earth's radiation belts are summarized in Table 2 and Fig. 1 [4].

Table 1 Proton dose rate in the inner radiation belt as function of altitude

Orbit altitude (km)	Proton dose rate (Sv/day)		
	0°	45°	90°
300	0.05	0.05	0.05
500	0.16	0.16	0.16
2500–3000	110.00	26.00	18.00
7500	2.60	3.40	2.40

Table 2 Characteristics of the Earth's radiation belts

Particle	Energy	Extension (Earth radii)
Earth		
e^-	1 keV–7 MeV	1–10
p^+	1 keV–300 MeV	1–7

e, Electron; p, proton

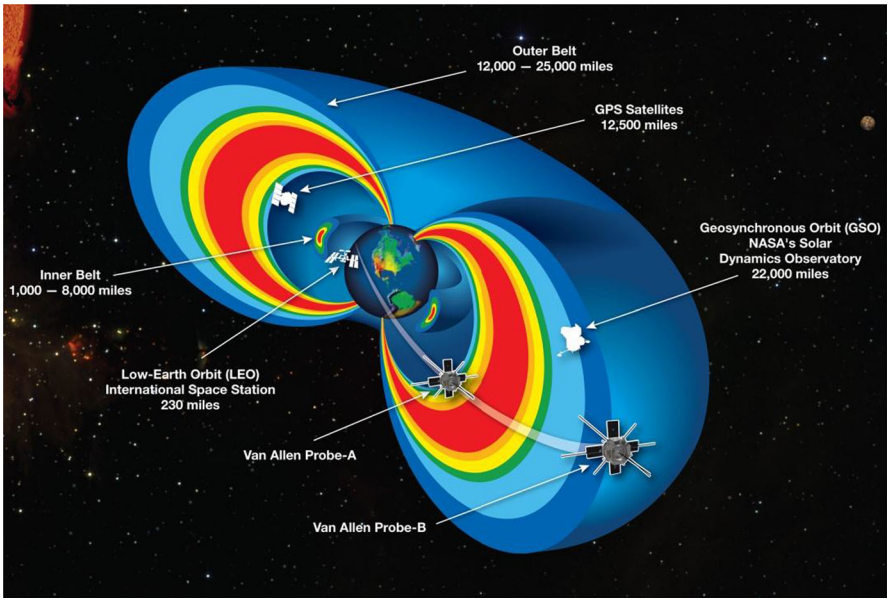

Fig. 1 Scheme of the Van Allen radiation belt. *NASA* National Aeronautics and Space Administration, *GPS* global positioning system

The Earth's magnetic field centre does not coincide with its geographical centre because the magnetic poles are not located on its geographic poles. Consequently, the Van Allen belts are slightly closer to the Earth on one side and slightly further away on the other side. They are closest to the South Atlantic area, which is known as the South Atlantic Anomaly (SAA), illustrated in Fig. 2, which has a relatively higher concentration of protons at lower altitudes (<1000 km). This asymmetry results in a spacecraft on an orbital flight being exposed to a much higher flux of protons when it passes through the SAA than when it passes though other locations at the same altitude.

2.2 Galactic Cosmic Rays

Cosmic rays were discovered in 1912 by Victor Franz Hess who, with the help of balloons, showed that ionization increases with altitude. Many years of research and the ability to get above the atmosphere, thanks to several space programmes, have provided evidence demonstrating that the Earth is bombarded by a nearly isotropic

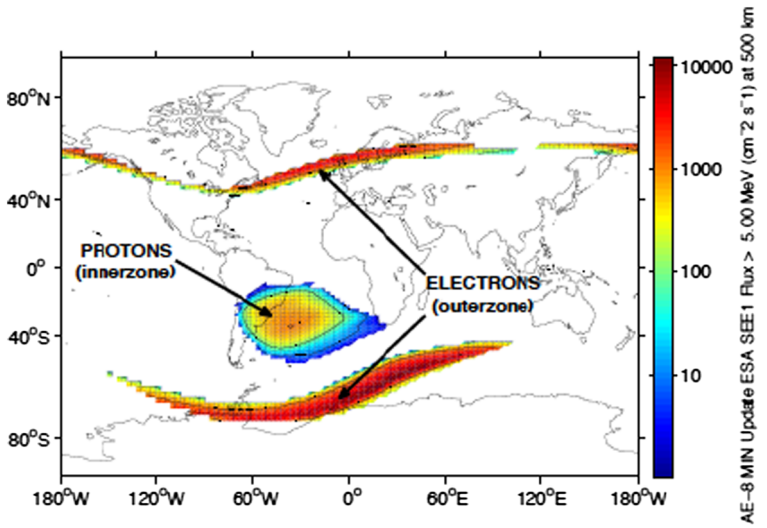

Fig. 2 Intensity of protons and electrons at an altitude of 500 km, estimated by AP8-MIN and AE8-MIN models, respectively [5, 6]. The South Atlantic Anomaly can be clearly seen in the Atlantic Ocean close to southeast coast of Brazil

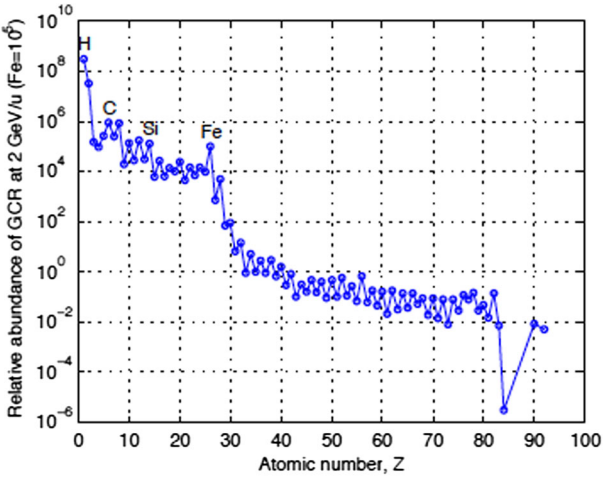

Fig. 3 Relative abundance of galactic cosmic rays (*GCR*) for different ion species at energies of about 2 GeV/nucleon as a function of the atomic number [8]

flux of energetic charged particles. Beyond the atmosphere, cosmic rays consist predominantly of protons (about 90%) and helium nuclei (almost 10%), but heavy nuclei are also part of the primary cosmic rays (Fig. 3).

Once these particles arrive in Earth's atmosphere, they interact with the nuclei of atmospheric molecules to form, in a cascade process, new particles that project forward, called secondary cosmic rays. Galactic cosmic rays (GCRs) travel at close to the speed of light, have huge energies (>GeV) and appear to have been travelling

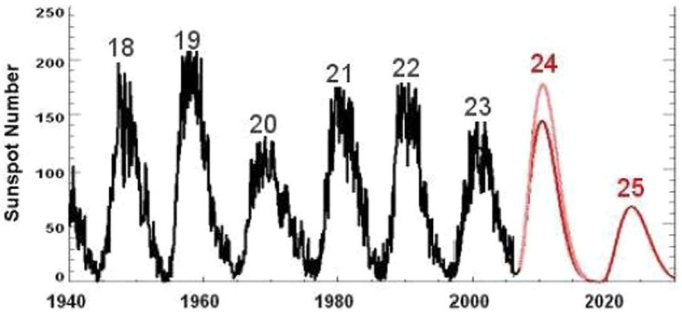

Fig. 4 Past and expected future sunspot numbers for solar cycles

through the galaxy for some ten million years before intersecting the Earth. They are partly deviated by the Earth's magnetic field and have easier access to the Earth at the poles compared with the equator. The Earth's surface is protected from these particles by geomagnetic shielding as well as by the atmosphere. The primary cosmic rays interacting with air nuclei generate a cascade of secondary particles comprising neutrons, protons, mesons and nuclear fragments. The intensity of radiation builds up to a maximum at an altitude of 18,000 m and then slowly drops off at sea level.

The penetration of these GCRs into the vicinity of the Earth is influenced by solar activity, which emits a continuous wind of ionized gas or plasma that extends beyond the solar system. The strength of the solar wind influences the flux of cosmic rays reaching Earth. This effect is referred as solar modulation and depends on solar activity. There is an 11-year cycle in solar activity, and we are currently experiencing a decreasing phase of solar cycle 24 (Fig. 4), with the last solar maximum having occurred in 2013, at which time the GCR were less intense.

The GCRs are a major radiation concern for long-term missions outside the Earth's magnetosphere. In addition, since they have high energies, most of them pass through the magnetosphere and are observed at LEOs. The flux of GCRs is therefore a possible hazard to spacecraft electronics because GCRs cannot be shielded due to their high energy.

2.3 Solar Cosmic Rays/Solar Particle Events

The solar wind mostly consists of high-energy electrons and protons, and the particle plasma of the solar wind travels through space at an average velocity of approximately 400 km/s. The average proton densities, in absence of any major solar events, are in the order of 1–10 protons/cm^3.

Intense magnetic activities are the origin of *Sunspots*, which are colder areas where the strong magnetic field blocks the transport of heat. The magnetic field also causes strong heating in the corona of the Sun, forming active regions that are the source of intense *Solar Flares* where huge amounts of plasma are ejected. The real massive solar flares are called *corona mass ejections* (CMEs). The CMEs are orders of magnitude larger than regular solar flares. In a CME event, a huge part of the

Sun's corona explodes, and matter of up to 10^{10} tons is ejected at velocities of up to thousands of kilometres per second [9].

Evidence has been found for particle acceleration processes throughout the heliosphere in the years around the solar maximum, in many cases in association with shock waves that are caused by the increasing number of solar flares and CMEs. Near solar maxima the Sun produces three to four CMEs every day, whereas near solar minima there is only about one CME every 5 days [10, 11]. CMEs are very unpredictable phenomena and responsible for the emission of mainly electrons and protons, but there are also heavier ions, such as oxygen and iron, present in the shockwaves. During these events very large amounts of energy can suddenly be released in the solar chromosphere through the ejection of accelerated particles into space. These different processes result in the generation of particles such as solar energetic particles with energies of up to about 10 MeV/nucleon, which accelerate in the solar corona and last a few days [12], and energetic storm particles with energies up to about 500 MeV, which accelerate in the propagating interplanetary shock and last a few hours [13], and anomalous cosmic rays (ACRs) [14]. Although the amount of heavier ions in the CMEs is much lower than that in the constant solar wind protons or electrons, they are more likely to be the cause of problems in the proper functioning of electronics due to their higher ability to ionize matter.

3 Interaction of Radiation with Matter

The production and type of radiation damage in matter is related to the energy deposition processes. The interaction of incoming particles with matter results in two major effects: (1) collision energy loss and (2) atomic displacement. Interactions of incoming particles and matter that result in the excitation or emission of atomic electrons are referred to as energy loss by ionization or energy loss by collisions with electrons. Non-ionization energy loss processes are interactions in which the energy imparted by the incoming particle results in atomic displacements or in collisions where the knock-on atom does not move from its lattice location and the energy is dissipated in lattice vibrations.

Defects induced by the interaction of radiation with semiconductors are primary point defects include vacancies and interstitials. Clusters of defects are generated when the incident particle, such as a fast neutron or protons, transfers enough energy to the recoil atoms to allow large cascades of displacements. The change observed in semiconductor conductivity is associated with the formation of defect clusters.

For charged particles, the amount of energy that goes into ionization is determined by the stopping power or linear energy transfer (LET) function, commonly expressed in units of megaelectron-volts square centimetre/gram (MeV cm^2/g) or more transparently as energy per unit length (dE/dx) in kiloelectron-volts per micrometre (keV/μm). The absorbed ionizing dose is the energy deposited per unit mass due to ionization, and the most common unit of measurement is the rad, which corresponds to 100 ergs/g. Because the energy loss per unit mass differs from one material to another, the material in which the dose is

deposited is always specified [e.g., rad(Si) or rad(GaAs)]. The Système International (SI) unit for dose is the gray, which is equivalent to 100 rad.

The LET or the rate of energy loss, dE/dx, for a charged particle passing through matter can be expressed approximately by $dE/dx = f(E)\cdot MZ^2/E$, where x is the distance travelled in units of mass/area or density × distance, $f(E)$ is a very slowly varying function of the ion energy E, M is the mass of the ionizing particle, and Z is the charge of the ionizing particle. Thus, for a given energy, the greater the mass and charge of the incident particle, the greater the amount of deposited energy produced over a path length inside the solid state material. For relativistic ions, the mass factor in the above equation becomes almost constant, and the ion charge dominates.

The intensity of heavy cosmic rays as a function of Z peaks at iron ($Z = 26$), abruptly decreasing thereafter. An energetic iron nucleus of 1 GeV per nucleon produces ~0.14 pC in each 10 μm of silicon traversed (the energy release of 22.5 MeV produces 1 pC of charge in silicon).

4 Space Product Assurance

4.1 Understanding the Problem

The integrated circuits required for applications in the space scenario are quite unique. Since silicon processes are a major corporate prerogative, companies involved in producing such processes serve a very large market. All technological and scientific efforts are focussed on applications that meet the consumer market, including such products as mobile phones, personal and notebook computers, among others. The benefits of a strong research in silicon processes, including size reduction (transistors channel length) and enhanced performance (clock speed), are reflected in more compact and more power final products.

Space electronics is a niche market, but one which has high-level requirements that basically are not satisfied by standard consumer electronics. The first and most important requirement is resistance to radiation, but resistance to both mechanical stresses (during launch) and thermal stresses is also relevant. Due to the low volumes required by the space market, large silicon foundries, do not always meet these requirements, resulting in basic technologies that are not suited for space. Consequently, there is a lack of technologies for the space environment.

Another aspect to be emphasized is linked to the availability of certain dedicated technologies developed for the military industry. Some silicon foundries in the USA (e.g. American Semiconductor Inc., Boise, ID) have developed silicon processes with a given resistance to radiation that are used in device design for military applications. The main problem related to this reality is that these players can only work for the military establishment and cannot provide either their components or their technology to markets outside of the USA. This policy is encoded in a set of rules called the International Traffic in Arms Regulations (ITAR) which controls the export and import of defence-related articles and services. ITAR was established during the Cold War, and its regulations were reinforced after 11 September 2001. It

restricts all base technologies which can be used for weapon building, including fighter planes and personal equipment for soldiers. Resistance to radiation of all forms is obviously considered in these technologies, and silicon processes for integrated circuits realized for the military market fall under ITAR restrictions. The space and the high-energy physics markets unfortunately are disadvantaged by this approach, the consequences of which are, from the point of view of silicon processes, that on the one hand there is a basic shortage of radiation technologies and, on the other hand, when a technology is developed it can fall under ITAR restrictions and therefore also be unavailable.

The ESA and all European large-scale integrators encounter difficulties in acquiring the essential components and technologies for the production of silicon processes, which is why they are pushing for ITAR-free technologies—i.e. a set of base and critical technologies which could be freely used by ESA members and their providers and integrators. A major aim of ESA is to develop a base technology internally (meaning in Europe) that will not fall under ITAR restrictions or any other restrictions.

A key feature of integrated circuits destined to be used for space applications is that of radiation tolerance. Beyond the atmosphere, many particles (electrons, protons and high-energy ions) collide with silicon devices used in the space environment, such as electronic equipment for satellites, probes or, in general, all spacecraft, releasing energy and possibly disrupting their operation.

There are two main effects of radiation on silicon devices:

- Long-term effects [total ionizing dose (TID) and displacement damage (DD)]
- Short-term and random effects [single-event effects (SEE)].

TID and DD result in progressive degradation of the devices, with the chip progressing to a state of general malfunction after months or years. SEE, is strongly dependent on the amount and nature of the energized particles, and in the worst case scenario such effects can be destructive.

Even though these problems have been carefully studied since the 1960s, very few devices have been designed to be rad-hard, primarily due to the fact that the space market represents only a small niche in the overall silicon market. The volumes needed for silicon devices of this nature are very low, while silicon foundries are structured to make a profit on devices designed for mass production. Moreover, the realization of devices of this kind is challenging due to the technology efforts needed to manufacture these products in a process line that is finely tuned to be quick and reactive to a continuously changing consumer market.

Nevertheless, some players do develop and produce rad-tolerant or rad-hard devices. For the most part, these devices are commercial, with a high level of die qualification and redundancy. More than one chip (usually ≥ 3) is mounted on the same board, and by using a voting method an amount of functioning errors is avoided. Moreover, the space market generally uses "old technologies" in order to take advantage of well-established techniques of both the process and the design arms, but this also leads to delay in the introduction of new technologies, or no introduction at all, which can be profitable as well. Table 3 summarizes the responsible sources of radiation damage, the elementary particles involved and the relative energy range.

Table 3 Space radiation sources, energies and relative effects on microelectronics

Radiation source	Particle	Energy range	Radiation damage
Radiation belts	Protons	Few keV–500 MeV	SEE → stochastic effect
			DD → cumulative effect
			TID → cumulative effect
	Electrons	Few eV–10 MeV	TID → cumulative effect
Solar flares	Protons	Few keV–500 MeV	SEE → stochastic effect
			DD → cumulative effect
			TID → cumulative effect
Galactic sources	Protons and HZE ions	Up to 300 MeV/amu	SEE → stochastic effect

HZE high-energy, high-charge nuclei component of galactic cosmic rays, *SEE* single-event effects, *DD* displacement damage, *TID* total ionizing dose

4.2 Total Ionizing Dose

The TID is a long-term degradation of electronics due to the cumulative energy deposited in SiO_2 or other dielectrics. Significant sources of TID exposure in the space environment include trapped electrons, trapped protons and solar protons. Simulations are used to determine the dose received by an electronic component as a function of equivalent aluminium (Al) shielding for a given mission, as the one shown in Fig. 5. In this example, the electrons of the Van Allen Belts dominate the contribution to TID until about 6–7 mm of equivalent Al shielding and then are nearly completely eliminated after 1 cm.

When incident radiation enters a semiconductor solid material, such as silicon, an electron–hole pair may be created if an electron in the valence band is excited across the band gap into the material's conduction band. Electron–hole pairs generated in the gate oxide of a metal-oxide semiconductor (MOS) device, such as a transistor, are quickly separated by the electric field within the space charge region. The electrons quickly drift away, while the holes of lower mobility drift slowly in the opposite direction. Oxides contain a distribution of sites, such as crystalline flaws, that readily trap the slow holes. Portions of the positively charged holes are trapped at the sites as they slowly flow by. The main degradation mechanism induced by total dose in MOS devices is caused by radiation-induced charge build-up in its gate oxide. Oxide-trapped charge in thicker gate oxide can invert the channel interface, causing leakage current to flow in the OFF state condition ($V_{GS} = 0$ V) (Fig. 6). For advanced integrated circuits (ICs) with thinner gate oxides, such as complementary metal–oxide semiconductor (CMOS) technology, radiation-induced charge build-up in field oxides normally dominates the radiation-induced degradation of ICs and induces large leakage currents.

The response of MOS devices to TID is complex because of the competing effects of the oxide trap and interface trap-induced threshold voltage shifts, which can change over time. The net result is that the behaviour of the IC is changed because of the induced charge build-up.

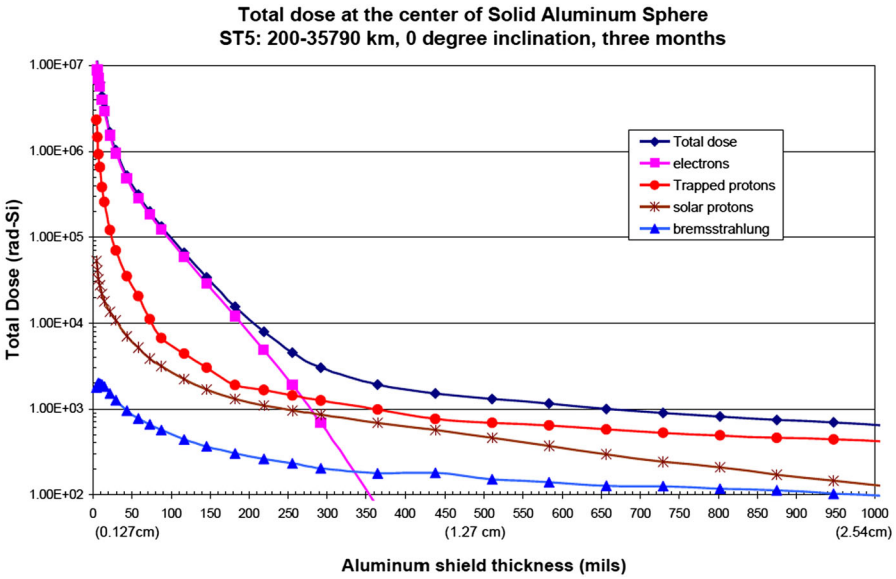

Fig. 5 Example of a dose as a function of the equivalent aluminium shielding

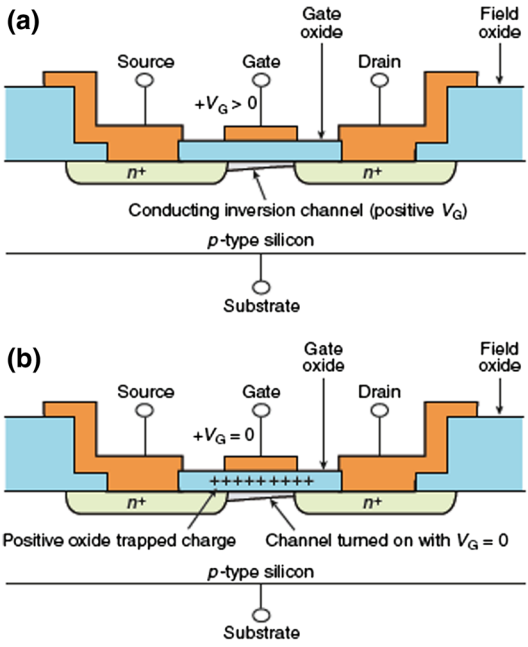

Fig. 6 Basic effect of total ionizing dose in a *n*-channel metal oxide–semiconductor field-effect transistor (MOSFET) inducing charge build-up in gate oxide. Normal operation (**a**) and post-irradiation (**b**) operation show the residual trapped charge (*holes*) that produces a negative threshold voltage shift

Electrical properties of CMOS, silicon-on-insulator (SOI) and bipolar technologies degrade with the cumulate dose because they are SiO_2-based devices. Typical effects include parametric failures or variations in device parameters, such as

leakage current, threshold voltage, among others, or functional failures. The gain degradation is the primary effect with bipolar technologies and is particularly large at a low bias level (Fig. 7). The gain decrease is due to an increase in the base current resulting from the degradations of the current that are caused by recombination in the emitter–base depletion region and the current due to recombination in the neutral base.

Bias and quiescent currents also commonly increase over the time of a spacecraft mission because of TID. In some cases, the increase in leakage current requires designers to add a significant margin to their power requirements. It is not uncommon for devices to show an order of magnitude increase in the leakage current as a result of TID while otherwise still functioning properly.

Satellite mission duration may extend over years, so a large TID may be accumulated during this time. Changes in the fabrication of ICs over the last decade have led to the development of a number of components with an enhanced sensitivity to radiation when exposed to low dose rates. Bipolar technologies are sensitive to the enhanced low dose rate sensitivity (ELDRS); in other words, the degradation at the end of a low dose rate (LDR) irradiation is greater than the degradation measured after irradiation to the same dose level obtained with a high dose rate (HDR).

The standard TID dose rate for ground testing is generally $\sim$50 rad/s. This dose rate allows a qualification test to be run in an 8-h shift. However, typical ELDRS testing is performed at a dose rate of only 10–100 mrad/s: therefore, there is a requirement for test times on the order of weeks to months, which is clearly much closer to the rate at which TID will be accumulated during the mission. This extended but more realistic testing is expensive and can affect a spacecraft programme mission schedule. Fortunately, some vendors producing radiation-hardened devices have determined the underlying cause of ELDRS for their parts and modified their manufacturing process to overcome the problem.

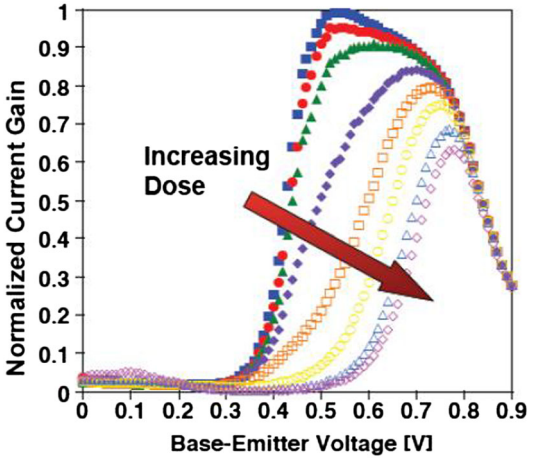

Fig. 7 Normalized current gain vs. base-emitter voltage for an npn bipolar junction transistor irradiated to various total doses

4.2.1 DD Dose

The long-term degradation characteristics of displacement damage dose (DDD) are often similar to those of TID, but the physical mechanism differs. It should be noted that technologies that are tolerant to TID are not necessarily tolerant to DDD.

DDD is essentially the cumulative degradation resulting from the displacement of nuclei in a material from their lattice position. Over time, sufficient displacement can occur and may change the device or the performance of its material properties. Prime sources of DDD exposure include trapped protons, solar protons and, to a less extent for typically electronic systems, trapped electrons.

Devices that depend on a crystalline bulk structure for operational characteristics, such as solar cells, particle detectors, image sensors, photonic and electro-optic components, have shown sensitivity to high DDD. Radiation particles, such as neutrons, protons and electrons, scatter off lattice atoms, locally deforming the material structure. The band–gap structure may change, affecting fundamental semiconductor properties. For example, the output power of a spacecraft solar array degrades during the mission life of a spacecraft because of the displacement damage. Another example of displacement damage is the increase in recombination centres in silicon particle detectors, ultimately leading to a signal and an energy resolution decrease.

Displacement damage is also important for photonic and electro-optic integrated circuits, such as charge-coupled devices and opto-isolators. Elastic and inelastic nuclear scattering interactions produce vacancy/interstitial pair defects as the regular structure is damaged. The defects produce corrupting states in band gaps, leading to increased dark current and reducing gain and charge transfer efficiency.

The amount of displacement damage is dependent on the incident particle type and energy, as well as on the target material. The characterization of displacement damage is more complex than characterization of TID. The most commonly used method to quantify displacement damage is non-ionizing energy loss (NIEL). NIEL coefficients vary depending on radiation type, energy and the target material.

The NIEL of a particle is usually presented in terms of kiloelectron-volts square centimetre per milligram or megaelectron-volts square centimetre per milligram . For a mono-energetic beam, the product of the NIEL with the particle fluence gives the DDD, which is usually specified in units of kiloelectron-volts per gram or megaelectron-volts per gram. For irradiation by a range of particle energies, the displacement damage dose is obtained by integrating the energy-dependent NIEL over the particle spectrum. Alternatively, a displacement damage equivalent fluence can be defined. This is the fluence of particles at a particular energy that would give an equivalent DDD. Often 10-MeV protons or 1-MeV neutrons are given as the reference. The values for the NIEL of various particles in silicon have been published by Dale et al. [15], Huhtinen et al. [16], Akkerman et al. [17], Summers et al. [18], with an online compilation by Vasilescu and Lindstroem [19]. Values are summarised in Fig. 8. Various calculations tend to agree within a factor of two, which is comparable with the uncertainties involved.

Values for InGaAs have been published by Walters et al. [20] and Fodness et al. have published results for HgCdTe [21]. Jun et al. have published results for protons

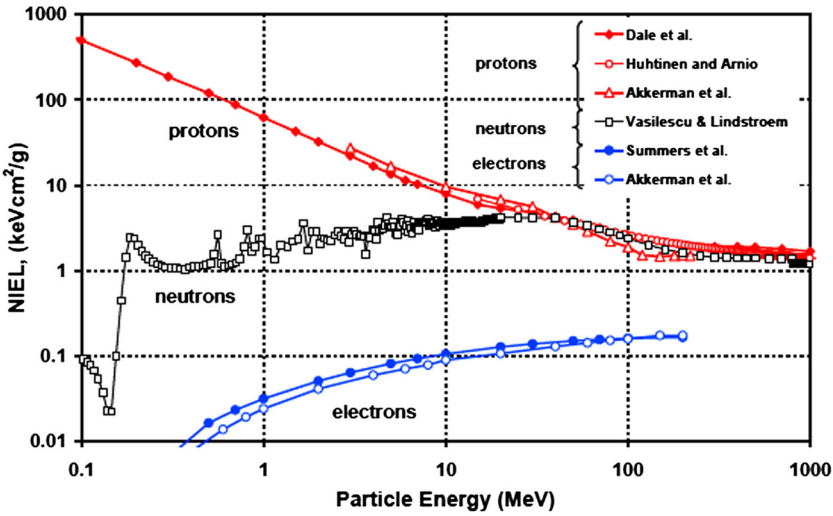

Fig. 8 Published values of non-ionizing energy loss (*NIEL*) in silicon

in a range of important semiconductor materials [22] and also for electrons [23] (Fig. 8).

4.2.2 Single-Event Effects

Single-event effects occur when a single ion strikes a material, depositing sufficient energy through its primary interaction (e.g. direct ionization of a GCR), or as a result of the secondary ions that occur from the strike induced by neutrons or protons (indirect ionization) to cause an effect in the device.

SEEs are generated by several mechanisms. The charge-collection mechanisms are an interesting and complex set of mechanisms that are continuously being refined in the literature. The charge generated by a single ion strike is collected, producing a spurious voltage signal on a "sensitive" node that causes an effect at the circuit level. The number of electron–hole pairs generated is proportional to the electron stopping power of the incident particle in the target material. The generated charge recombines or is collected at the various nodes. The charge collection threshold for a SEE is called the critical charge (Qcrit).

SEE tests are performed at particle accelerators. SEE sensitivity is characterized by the cross-section σ as a function of the LET,

$$s = \frac{N}{F},$$

where N is the number of SEE events and Φ is the particle fluence.

The LET can be varied at a particle accelerator by changing the incident particle mass, incident energy and angle of strike. A particle impinging on a device at 60° will deposit twice the energy of a particle entering at normal incidence, thereby effectively doubling the LET:

$$\mathrm{LET}(q) = \frac{\mathrm{LET}(0^{\circ})}{\cos(q)}$$

The key measurement for these experiments is the number of single events that occur as a function of the number of incident particles at a given LET. These data are combined with spacecraft trajectory information and are used to predict a specific mission SEE rate.

The many SEE types can be divided into three basic categories [24, 25]:

- Single-event upset (SEU) and multiple bits upset which change the logic state of the internal nodes of a circuit. These errors are called soft error and are recoverable.
- Single-event latch-up (SEL), in CMOS technologies, which may destruct the circuit if SEL is not interrupted within a short time when it occurs.
- Single-event gate rupture/burnout (SEGR/SEB) in power metal oxide–semiconductor field-effect transistor (MOSFET), which causes failure or destruction of the transistor.

4.2.2.1 Single-Event Upset A SEU is the change of state of a bistable element, typically a flip-flop, or of another memory cell that is caused by the impact of an energetic heavy ion or proton. The effect is non-destructive and may be corrected by rewriting the affected element. As with other SEEs, a single-particle strike may introduce sufficient charge to exceed the Qcrit of a sensitive circuit node and change the logic state of the element. The resulting change of state is often known as a bit-flip and can occur in many different semiconductor technologies.

The vulnerability of a device to a SEU is determined by two parameters: the threshold LET, which is the minimum amount necessary to produce upset, and the saturation LET cross-section (in cm^2), which is a function of the surface area of all of the SEU-sensitive nodes.

Static random access memory (SRAM) and dynamic random access memory (DRAM) are two common integrated circuit memories that experience SEU. SRAM structures consist of an array of nearly identical memory cells, and DRAM structures have cells that use the charge storage in a capacitor to represent data. Both types of memory circuits also include supporting circuitry, such as sense amplifiers and control logic, that also may be sensitive to SEEs or single-event transients (SETs). Very dense memory circuits may also have multiple bit upsets when one ion strike causes upsets in multiple bits, which may occur if the ion track is close to both bits or if the angle of incidence is close to parallel to the die.

SETs are short-time voltage excursions at a node in an integrated circuit caused by a transient current generated by the nearby passage of a charged particle. Most SETs are harmless and do not affect device operation. However, there are several types of SETs that can cause harm or corrupt data.

SEUs or SETs are not directly observable at the pins of a device. However, at some time after a SEU or SET occurs, the device may operate in an unpredictable manner. Single-event functional interrupts (SEFIs), a class of SEEs,

have been observed in complex devices, such as microprocessors or flash memories. A SEFI is a SEE that places a device in an unrecoverable mode, often stopping the normal operation of the device. It is usually caused by a particle strike but can be produced by other causes. SEFIs are not usually damaging but can produce data, control or functional-interrupt errors which require a complex recovery action that may include reset of an entire spacecraft subsystem.

4.2.2.2 Single-Event Latch-up Transient currents generated by ionizing particles can be amplified by parasitic devices forming a latch-up. A SEL causes the loss of device functionality due to a single event-induced current state [26–28]. SELs can result in permanent damage to the circuit that may not be recoverable [29]. SEL can occur in any semiconductor device that has four layer parasitic PNPN paths, which can be triggered by transient currents. Many techniques have been proposed to overcome latch-up by using current sensing circuits, which can be used to temporarily switch off the power supply. The removal of power should be done within milliseconds after development of the latch-up condition to avoid possible damage to the circuit. SELs do not occur in SOI technology due to its nature preventing the presence of the parasitic PNPN structure [30].

4.2.2.3 Single-Event Gate Rupture/Burnout Power devices may be sensitive to SEB and SEGR. SEB is similar to SEL in that it generates high-current states that ultimately lead to catastrophic device failure. SEB is a high-current condition in a parasitic npn bipolar structure similar to latch-up. It is observed in vertical power MOSFETs and some bipolar transistors. The charged particle strike induces current in the p-structure forward-biased parasitic transistor. If the drain-source voltage is higher than the breakdown voltage of the parasitic npn, an avalanche occurs and high current flows. This effect can be permanently damaging for one or more of the parallel islands in the architecture of the power MOSFET by producing an uncontrolled short.

SEGR is initiated when the incident particle forms a conduction path in a gate oxide, resulting in device damage (Fig. 9). SEGR can occur when charge builds up in dielectric around the gate of a power MOSFET when a large bias is applied to the gate. The localized field builds up enough for the field across the dielectric to exceed the dielectric breakdown voltage, resulting in a low-resistance path across the dielectric. The conduction path in the oxide is an example of classic dielectric breakdown similar to lightning during a thunderstorm.

4.3 Radiation Hardness Assurance Testing

The radiation endurance of electronics operating in a harsh radiation environment needs to be assured either by manufacturing them (Rad-Hard) or by testing them. Because of high production costs, the Rad-Hard industry is mainly focussed on parts with high reliability requirements. In addition to lower prices, the performances of commercial electronics [commercial-off-the-shelf (COTS)] is typically much higher than that of Rad-Hard devices. Thus, COTS are often favoured in space projects due

Fig. 9 A catastrophic single-event gate rupture in a power metal oxide–semiconductor field-effect transistor causing functional failure

to superior performances and low cost. However, the drawback is their lack of being "space-qualified" and unknown radiation performances.

4.3.1 TID Testing

Although the space environment has a low dose rate ($\sim 10^{-4}$–10^{-2} rad/s), the duration of missions may be in years, thus resulting in large accumulated doses. Over the life of a spacecraft mission, TID levels on the order of 10^5 rad are easily accumulated. Candidate devices need to be characterized and qualified with respect to the requirements of a spacecraft mission.

The total dose test consists of exposing the selected device to ionizing radiation while appropriately biased and then performing a set of electrical measurements either during or after irradiation. One approach, called step-stress, consists of measuring electrical parameters after a dose of ionizing radiation has been reached and determining their changes with respect to the initial measurements. An other approach, called in-flux testing is performed by continually measuring the device response as it is being irradiated. The step stress approach is usually more convenient and much more widely used.

The test is performed with different samples of the same type exposed at same time at a number of accumulated dose levels. Generally the ionizing radiation environment is simulated with 1.25-MeV gamma rays from Co^{60} (Fig. 10) sources even though the radiation space environment responsible for TID consists primarily of electrons and protons of various energies. These sources can have a dose rate of up to 600 rad(Si)/s, but it is possible to decrease the dose rates by varying the distance from the source or varying the thickness of absorbing materials.

Since the parts of any device are used under different conditions in a spacecraft, they are generally biased during testing in the condition that gives the worst-case damage.

Standard procedures have been developed in the USA (MIL-STD 1019.5 [31] and ASTM F1892 [32]) and in Europe (ESA/SCC 22900 [33]). These standards define the requirements applicable to the irradiation testing of integrated circuits and

Fig. 10 ^{60}Co radiation sources for low and high dose experiments

discrete semiconductors. The MIL-STD 1019.5 procedure was written for military applications and has been adapted for space applications. The European procedure is only applicable to space applications. Both procedures define the test conditions in order to obtain a conservative estimate of the radiation sensitivity of parts of CMOS devices, but in different ways. The dose rate to be used during test is, following ESA/SCC22900, 1–10 rad/s for the standard window and 0.01–0.1 rad/s for the low dose rate window.

The dose to the device under test (DUT) has to be measured alternatively by the appropriate detector (dosimeter or ion chamber) by correcting a previous dosimeter measurement for the decay of ^{60}Co source intensity in the intervening time.

A proper calibration of the source is crucial before any radiation testing is started. Several organizations use different approaches to calibrate their sources. However, the general recommendation is the guarantee of the uniformity of the radiation field in the volume in which the devices are irradiated within a few percentage points of accuracy.

Many ionization chambers are available for the measurement of the dose. Typically, those of smaller volume are used for HDR calibration (e.g. 0.18 cc) and those of higher volume are used for LDR calibration (e.g. 180 cc).

The dose level at which a part must to be subjected is often dependent on the project requirements. Several missions require testing to the exact dose of the mission plus a margin factor, typically 2 or 3. High-dose missions sometimes require testing to failure in order to obtain maximum leverage of the capabilities of the part before establishing the radiation guideline.

Another common type of laboratory source is the 10-keV X-ray source. Laboratory X-ray sources are available that can achieve dose rates from $<$300 rad(Si)/s to $>$3600 rad(Si)/s. These sources can be used to irradiate both unleaded packaged devices and devices on a wafer. The HDR of X-ray sources and the capability for testing at the wafer level allows for rapid feedback on radiation hardness during device fabrication [2]. However, these sources are not recommended for radiation qualification.

Two HDR sources can be used to investigate the total dose response of electronic devices at short times: these are electron linear accelerators (LINACs) and proton cyclotrons. Electron LINACs are pulse-type sources with pulse widths ranging from

<20 ns to >10 μs with energies from 10 MeV to >40 MeV. Proton cyclotrons are quasi-continuous sources and can have dose rates from a few rad/s up to high-dose rates [1 Mrad(Si)/s] with energies from around 20 MeV to >200 MeV.

4.3.2 DDD Testing

Ideally, for mission evaluation, the devices under test should be irradiated with particles and energies representative of the operating environment to avoid uncertainties in the NIEL approach. An approximation of the proton for low Earth orbits can be simulated using a selection of proton beam degraders and sequential irradiations. The main focus of interest is protons with energies of several tens of megaelectron-volts as the shielded spectrum usually has a peak at around 50–60 MeV, with 10-MeV protons sometimes used for convenience because of beam availability or activation issues.

Also, care must be taken if proton irradiations are being used for a combined test of TID and displacement damage effects. At these low energies intracolumnar recombination of the generated electron hole pairs become significant, leading to a lower degradation due to TID than would be expected if irradiating with ^{60}Co gamma or higher energy protons.

Neutrons are sometimes used for space simulation to avoid ionization effects that occur when irradiating with charged particles. One possible problem with neutron irradiation is that the energy spectrum is normally not mono-energetic and the dosimetry and application of NIEL can be complex.

Knowledge of the actual energy spectrum of the particles incident on the device is very important for fundamental studies. Using a tuned beam to obtain mono-energetic protons is preferable to using degraders to obtain the required proton energy. The beam energies of degraded beams have significant straggle that can complicate the data analysis. For example, the Proton Irradiation Facility (PIF) at the Paul Scherrer Institute (PSI) provides 13.3-MeV protons with a full width at half maximum of 5.6 MeV by using a 74.3-MeV beam reduced with Copper degraders. It is particularly important for low-energy irradiations that the effects of any material in front of the die be understood, including the device package.

The proton flux is usually selected to ensure that the time required to reach a specified fluence is within acceptable practical limits and to minimize beam time, but not too high so that dosimetry and radioprotection become problematic. In practice, proton irradiations for displacement damage testing are normally performed with fluxes in the range 10^7–10^8 p/cm^2/s.

The initial defect concentrations produced by displacement damage are usually considered to be independent of bias applied during irradiation. Therefore, displacement damage testing is usually undertaken unbiased. Unbiased irradiations tend to lead to a reduction in the effects of TID and, therefore, displacement damage effects can be isolated more easily.

Beam uniformity information should be available from the irradiation facility, and the level of uniformity should be appropriate for the required testing. If the uniformity is marginal, for example if the device under test is particularly large in relation to the specified beam diameter, or if several devices are being irradiated at

the same time, the beam should be characterized prior to irradiation testing being undertaken. There are several ways in which the uniformity can be determined, such as by using a radiochromic film or a scanning photodiode. Once the beam uniformity has been determined the device under test should be carefully aligned to the centre of the beam where the uniformity is likely to be optimum.

4.3.2.1 Proton Sources Most proton irradiation facilities supply protons through the use of particle accelerators, such as tandem Van de Graaff generators, cyclotrons or synchrotrons. Linear accelerators are also employed occasionally. Many such particle accelerators are used for medical or industrial purposes and may not always be available for device testing. Most Tandem Van de Graaff-based facilities provide protons having energy of up to $\sim$10 MeV. Some facilities do provide protons with higher energies, such as the SIRAD-INFN facility in Italy, which provides protons of up to 30 MeV. Generally the beam sizes tend to be a maximum of a few centimetres in diameter, although the maximum irradiated area can be sometimes increased through the use of scanning techniques. Cyclotrons tend to be employed when protons of higher energies are required. Typically energies of up to a few tens of megaelectron-volts are available from these facilities, but some offer protons with energies as high as 200 MeV. For example, the cyclotron at the Université Catholic de Louvain, Belgium, provides protons with energies of up to 62 MeV and the high-energy beam line at the PSI in Switzerland supplies protons with energies of up to 250 MeV. Beam diameters of 10–20 cm are typically available. If proton energies are required below the maximum energy that is available, energy reduction is possible by either tuning the beam or using degraders. Degraders are material plates, usually aluminium, that are placed between the beam and the device under test, with the material and thickness of the plate being chosen to achieve the required energy. Although convenient, degraders should be considered with care because although the mean energy will be reduced, the straggling causes a broadening of the energy spectrum that may result in a more complex analysis of the test results.

4.3.2.2 Neutron Sources Neutrons for device testing can be supplied from radionuclide sources, from nuclear reactors and from nuclear reactions produced with particle accelerators. The most commonly used spontaneous fission source is the radioactive isotope Californium-252, which produces a spectrum of fission neutrons that peak at 1 MeV and extend out to $\sim$13 MeV (Fig. 4). Alpha reaction sources are also used, such as the americium–beryllium or americium–lithium reaction. Mono-energetic neutrons can be provided by using the deuterium–tritium (14.1 MeV) or deuterium–deuterium (2.5 MeV) reaction. Such facilities are available at, for example, the Atomic Weapons Establishment in the UK or the Fraunhofer Institute in Germany. High-energy neutrons are available from nuclear spallation facilities where a high-energy proton beam, produced by a cyclotron or synchrotron, for example, impacts target material, such as Tungsten. The neutron energy extends from thermal up to the energy of the incident proton beam. For example, the spallation source at the Svedberg Laboratory at Uppsala University,

Sweden provides neutrons of up to 180 MeV. The quasi-monoenergetic neutron (QMN) facility at the same laboratory produces neutrons from accelerated protons incident onto a ^{7}Li target. The resultant neutron spectrum is dominated by a high-energy peak at an energy variable between 17 and 180 MeV.

4.3.2.3 Dosimetry

Faraday cup A Faraday cup has a shielded, insulated target block thick enough to stop the incident protons. The charge deposited in the block is measured (e.g. with an electrometer) and is proportional to the number of stopped protons. Electrostatic and magnetic fields are often used to suppress the current from external secondary electrons or to prevent secondary electrons generated within the cup from escaping. Faraday cups do not provide absolute real-time monitoring; they are moved in and out of the beam or are placed in a separate area to provide measurements only when needed for calibration of other detectors.

Scintillators A scintillator is a material which, when irradiated, converts a fraction of the interacting particle energy into light. The light output is proportional to the ionizing energy lost by the incident particle. The generated photons can be detected by a photomultiplier, avalanche photodiodes or silicon photomultiplier. These detectors can be used for real time monitoring of the flux and various arrangements can be employed.

Secondary electron monitors If an irradiating beam passes through thin metal films, such as aluminized Mylar, secondary electrons will be generated. If the films are connected to a picoammeter, the resultant current is proportional to the number of ions passing through the foil. This simple arrangement can be adapted by appropriately biasing and segmenting the foils to enable the determination of the beam uniformity and focus.

Radiochromic films Radiochromic films are frequently available for on-demand testing of a beam's uniformity in a purely qualitative manner. The film is exposed to a dose known not to saturate the film. The film is then read by any number of means, but the most popular method is to scan the film with a simple flatbed scanner into a gray scale (0–255) image and process it with a commercially available software package.

4.3.3 SEE Testing

In this case, the environment, due to high-energy GCR and solar event heavy ions, is simulated with low-energy ions available in particle accelerators. Each ion with a given energy is characterized by the amount of energy lost per unit length: the LET. Ground testing is performed with ions with lower energies than GCR or solar events but with similar LET. Commonly used specifications are reported by the Electron Industries Association [34] and ESA [35].

The typically used energy us of an order of several megaelectron-volts per micron, which means a penetration range in silicon from about 30 μm for heavy

ions to few hundreds of microns for the lightest particles. The device package in front of the die is removed for heavy ion SEE testing (Fig. 11).

Different values of LET are obtained by changing the ion species. A typical SEE test uses a minimum of five ion species in order to have a range of LET values from few megavolts per milligram square centimetre to about 60 MeV/mg cm^2. Typically high LET values are obtained by accelerating Xenon ions with a LET value of $\sim$60 MeV/mg cm^2. Higher LET values have been obtained or by tilting DUT or accelerating high Z heavy ions, such as gold.

In recent years several accelerators used for nuclear physics have been employed for the radiation hardness assurance test. In Europe, the most used facilities are the Accelerator Laboratory at the University of Jyvaskyla (JYFL), the so-called RADEF facility [36] (Fig. 12), and the cyclotron Cyclone 110 at Université Catholique de Louvain [37].

The single-event test consists of monitoring a certain number of parameters of a device during irradiation, detecting and counting the errors during each irradiation run. The SEE cross-section is measured as the ratio of the number of errors to the ion fluence expressed in particles per square centimeter. For devices that are sensitive to SEE even at low LET values, the test with a proton beam has to be also performed. In this case, since proton energy, as in space, is available at accelerators, the SEE cross-section is measured as function of proton energy. Typical values of ion fluences are 10^6 ions/cm^2 for soft errors and 10^7 ions/cm^2 for hard errors. The required ion fluxes ranged from 100 to 10^5 cm^{-2} s^{-1}. The number of soft errors are typically counted and stored. At the end of each run, the SEU cross-section per bit can be calculated by using the formula $\sigma_{SEU} = N_{SEU}/(\text{nbit} \cdot \text{Fluence})$. The characteristic SEU sensitivity of a device can be obtained by changing the LET using different accelerated ions. Moreover, LET can be varied by DUT tilting, which introduces the concept of effective LET, defined as $LET_{eff} = LET/\cos\theta$. In this case, the fluence must be corrected by multiplying by $\cos\theta$.

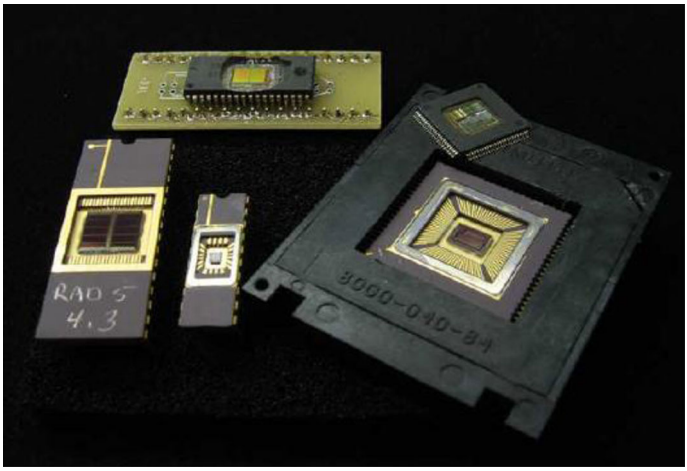

Fig. 11 Integrated circuits prepared for heavy ion testing by removing package lids or etching the plastic mold compound

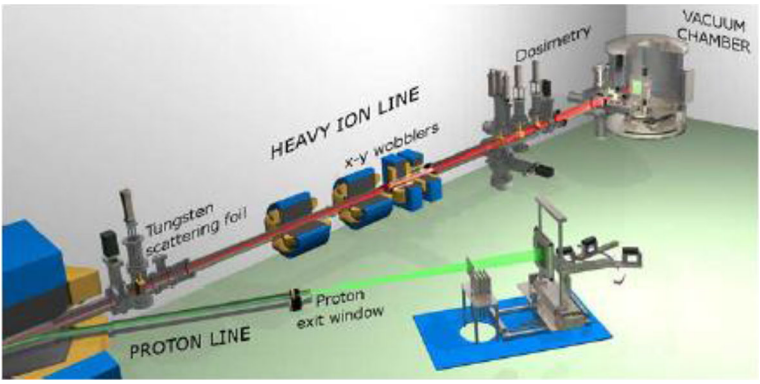

Fig. 12 Illustration for the overview of the RADEF facility (University of Jyvaskyla, Finland)

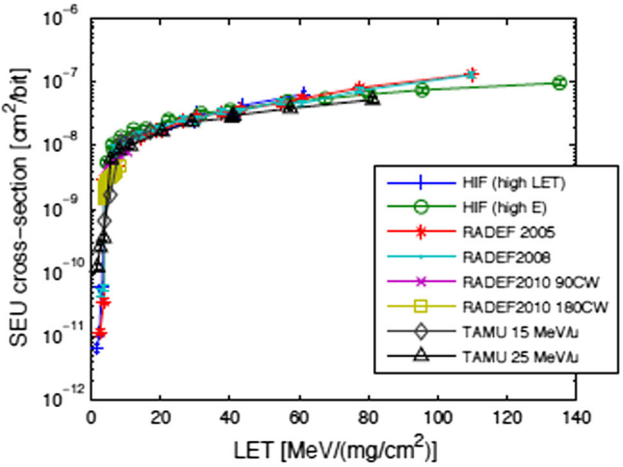

Fig. 13 Single-event upset cross-section for 4-Mbit Atmel AT60142F SRAM [39]

A typical SEU cross-section versus LET curve is reported for the 4-Mbit Atmel AT60142F SRAM in Fig. 13, which also shows the so-called SEU monitor [38].

This kind of characteristic plot can be used for estimating the SEU rates in the operational environment. The upset cross-section curve can be roughly characterized by a LET threshold and a saturation upset cross-section. To determine the number of circuit errors that will result during a space mission, one must convolve the upset cross-section curve with the heavy ion LET spectrum for the orbit (Fig. 14). This can be done by using dedicated software, e.g. CREME-96 [8], by assigning the environment and entering the parameterized SEU cross-section curve. From these input data the code will give estimation for the SEU rate in orbit.

In the case a device is sensitive to low LET values (<15 MeV/mg cm^2) a test with high-energy protons (in the range 50–250 MeV) is required in order to predict the SEE rate induced by protons in the mission environment. Direct ionization by

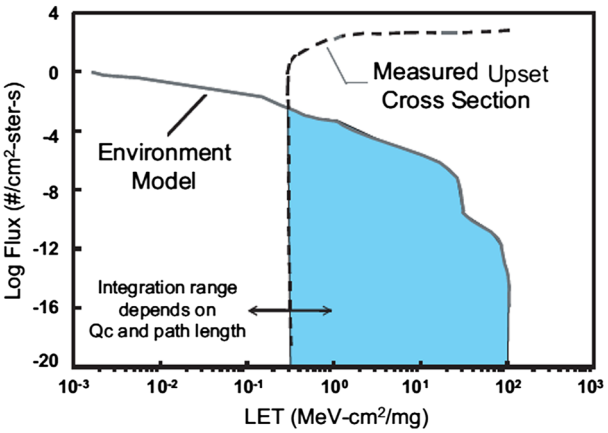

Fig. 14 Measured cross-section vs. linear energy transfer and particle flux for a hypothetical environment. The error rate is determined by convolving the environment model with the error cross-section

protons does not usually produce sufficient charge to cause SEEs. Protons and neutrons can both produce significant upset rates due to indirect mechanism. A high-energy proton may undergo an inelastic collision with a target nucleus. The reaction products, being much heavier and having high Z, can deposit a significant amount of charge. The proton SEE test requires large particle fluence (10^{10}–10^{11} protons/cm^2) to observe effects with statistical confidence. Because of this high fluence, tens of kilorad in terms of total dose can be accumulated by DUT. The dose level received by devices is monitored during the SEE test. In order to avoid damage to the DUT due to accumulated dose, new devices (not irradiated) are used during SEE test.

A SEL can occur during SEE test. A dedicated SEL test should be made under the condition of maximum power supply voltage. In most cases the See test involves power monitoring and the use of a control circuit during latch-up testing that allow power to be shutdown quickly after the latch-up is detected. Power after a sufficient time is restored. In the case of a high number of SEL, dead time has to be considered for a proper cross-section evaluation.

Successful SEE testing requires that the particle beam, whether composed of protons or heavy ions, can reach the sensitive regions of the device under test with minimal alteration from extraneous materials—e.g. air gaps, device packaging, semiconductor materials (substrate and back-end-of-line), among others. This criterion is generally not an issue for medium- and high-energy proton beams as their range is sufficient to penetrate large volumes of air, packaging and semiconductor materials, but it is critical for heavy ion testing due to the short range of these particles at most test facilities. Because of this, device preparation is an important step in conducting SEE testing and needs to be considered early in the test design phase.

The JEDEC, ESCC, and ASTM standards for the SEE test include provisions for beam uniformity and purity, but these are specific to spatial uniformity and ion

species. SEE testing and analysis techniques typically assume a monoenergetic beam or a beam with energy spread no more than a few percentages of the total kinetic energy. However, a heavy ion beam is often degraded to achieve different stopping powers.

Ion or proton beam dosimetry is one of most important issue in the SEE test. Several detectors positioned on the beam line can be used to monitor beam flux during the irradiation and certify the final fluence achieved. In some cases, photomultiplier tubes (PMTs) equipped with scintillator crystals are positioned at the edge of the beam in order to monitor it during the irradiation. Another possible solution is to use a gaseous detector as a parallel plate avalanche counter. This detector allows very high flux rates (up to 10^5 particles/s cm^2) to be counted and has the advantage that it can be placed in front of the beam with a minimal amount of degradation materials and no beam energy spread.

For all types of detectors, a calibration correction factor between the flux measured at the online dosimeter position and the flux at the DUT position has to be evaluated. This is done as a standard facility operation prior to starting the SEE test by measuring the flux with another detector placed at the DUT position and obtaining the correction factor.

Laser light is an easy way to induce SEEs in devices in laboratory. This technique proved to be very useful for SEE mechanism studies and SEE test setup debugging prior to performing the test at the accelerator. Laser light interacts in a very different way with the ions, and this interaction cannot be used to describe the in-orbit behaviour of a device. Laser data always need to be calibrated with heavy ion data.

4.3.4 Solar Cell Degradation

Space solar cells have been used as a power sources by satellites since 1954 [40], and they have played an important role in scientific research and space development applications. The objectives of research and development of space solar cells are to improve conversion efficiency, increase life time (radiation resistance) and reduce the mass and cost of solar cell.

The influence of Earth's radiation belts on satellite solar cells is primarily determined by protons and high-energy electrons (with the energy approximately 1 MeV).

Modern satellites need more electric power than previous ones because they have more challenging missions and require more equipment. Solar cells with high conversion efficiencies are required to keep weight and launch costs low. They are also required for outer space missions (i.e. far away from the Sun) where light intensity is lower. In this context, GaAs solar cells are promising for space applications due to their higher theoretical and practical efficiencies [41, 42] (28.3%) [43] in comparison to silicon cells [44], [45]. An additional benefit is the fact that the GaAs solar cells are more resistant to irradiation by energy electrons [45], [46] which introduces defects into solar cell structures. In semiconductors, radiation usually produces atomic displacements, which in turn result in the generation of lattice defects, such a vacancies, interstitials and complex defects [47].

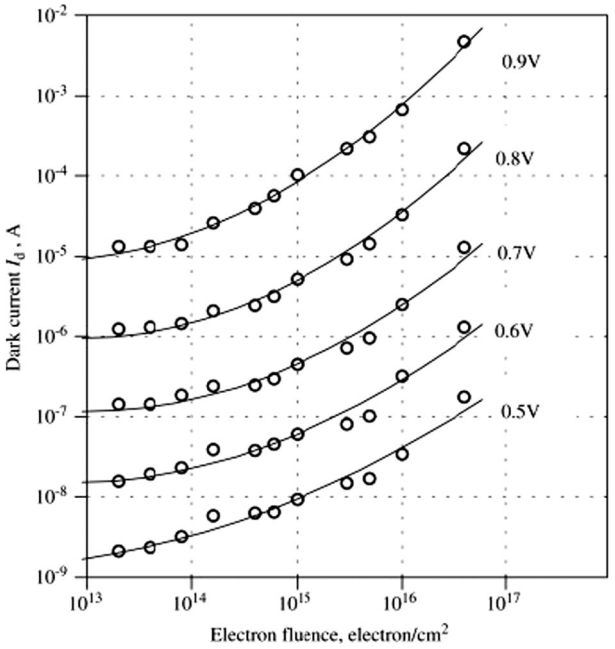

Fig. 15 The dark current as a function of the irradiation fluence for forward-biased cells

Lattice defects that act as recombination centres or trapping centres cause a decrease in the output power of solar cells.

Solar cells provide power on space vehicles for long-term operations in an environment that includes the electron and protons of the Earth's radiation belts. Satellites are often expected to function for periods as long as 10 years. For some orbits close to maximum flux levels the cells are exposed to an integrated fluence up to 4×10^{15} electrons/cm^2 with an effective energy of 1 MeV and 4×10^{13} protons/cm^2 with energies of between 1 and 80 MeV. All indications are that the changes produced in the cells are cumulative, and therefore it is prudent to assume that the changes in cell characteristics which will result after 10 years are about the same as those which would result from an equivalent integrated flux delivered at a much higher rate.

Electron irradiation typically has effect on dark current and short circuit current as reported in Figs. 15 and 16 [48].

In general, the electrical characteristics of solar cells are evaluated at a measurement facility before the cells are brought to an accelerator facility for irradiation (by protons or electrons) and subsequently returned to the measurement facility for re-measuring. However, this "sequential method" needs relatively high quantities of samples that can be irradiated by different amounts of electrons/protons with different accelerating energies to fully reveal the degradation of solar cells.

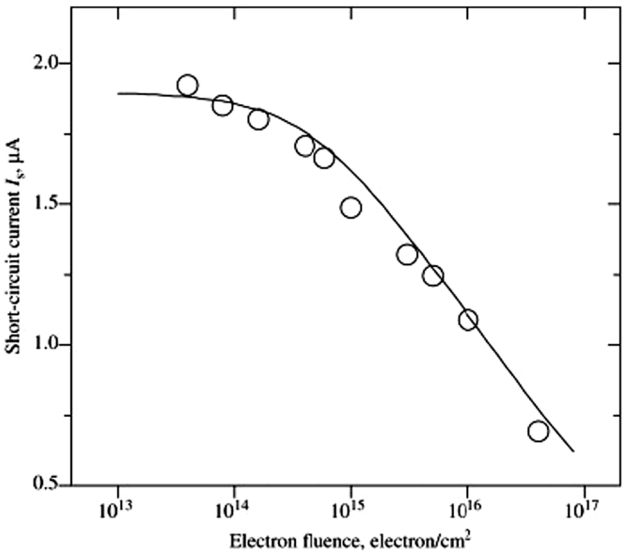

Fig. 16 The short-circuit current as a function of the irradiation fluence

For solar cells, the primary energy loss mechanism is through non-ionizing effects that lead to the displacement of atoms in the semiconductor lattice. The displacement of atoms results in lattice defects, such as vacancies, interstitials (displaced atoms moving to non-lattice positions), and to the formation of defect energy levels in the semiconductor material [49, 50]. These defects produce carrier-trapping centres (e.g. recombination centres and compensation centres) in the semiconductor bandgap and also generate carriers. Carrier generation leads to an increase in the forward bias dark *I–V* curve and degrades V_{oc}.

Recombination centres reduce minority carrier diffusion length, or minority carrier lifetime, and decrease the photovoltaic output of the cell. For GaAs and Si cells, radiation-induced recombination centres serve as the primary mechanism for the degradation of cell performance. The decrease in the minority carrier diffusion length degrades $I_{\text{short-circuit}}$ and leads to an increased forward biased dark *I–V* curve, which also degrades V_{oc}. In order to generate photocurrent output, charge carriers must diffuse to the junction before recombination occurs [51, 52]. Degradation of the minority carrier diffusion length reduces the cell's efficiency. For GaAs solar cells, the average diffusion length of the photo-generated carrier is large in comparison to the junction distance; for silicon cells, the average diffusion length is comparable to the thickness of the generating region of the photo-carrier. Thus, the decrease in diffusion length of carriers in silicon corresponds to a decrease in efficiency, whereas for GaAs solar cells, carrier diffusion length degradation contributes to a smaller decrease in efficiency.

Detailed treatment of radiation damage of solar cells from electrons and protons is reported on [7].

References

1. National Aeronautics and Space Administration (NASA) (1999) Space radiation effects on electronic components in low earth orbit. Lesson 824. Johnson Space Center, Houston. http://llis.nasa.gov/lesson/824. Accessed 23 Nov 2016
2. Van Allen L, Ludwig G, McIlwain R. Observation of high intensity radiation by satellites 1958 alpha and gamma. In: IGY Satellite Series, vol 3. National Academy of Sciences, Washington DC, p 73
3. Lang KR (2001) The Cambridge encyclopedia of the sun. Cambridge University Press, Cambridge
4. A travel in radiation activities through a Space program—Short course (2011) 12th European Conference on Radiation and its effects on Component and Systems (RADECS), Sevilla
5. Sawyer DM, Vette JI (1976) AP-8 trapped proton environment for solar maximum and solar minimum. NASA STIRecon Technical Report N, vol 77, p 18983. http://hdl.handle.net/2060/19770012039. Accessed 23 Nov 2016
6. Vampola AL (1997) Outer zone energetic electron environment update. In: Proceedings of the IEEE conference on high energy radiation background in space, p 128–136
7. SPENVIS Collaboration. The space environment information system, 1997–2009. http://www.spenvis.oma.be. Accessed 23 Nov 2016
8. The CREME Collaboration. CREME-MC. https://creme.isde.vanderbilt.edu. Accessed 23 Nov 2016
9. Jokipii J, Sonett C, Giampapa M (eds) (1997) Cosmic winds and the heliosphere. Space Science Series. Tucson, University of Arizona Press
10. Andrews MD (2003) A search for CMEs associated with big flares. Sol Phys 218:261–279
11. Ramesh KB (2010) Coronal mass ejections and sunspots—solar cycle perspective. Astrophys J Lett 712:L77–L80
12. Gabriel SB (1998) Cosmic rays and solar protons in the near earth environment and their entry into the magnetosphere. ESA Workshop on Space Weather, ESTEC, The Netherlands, Noordwijk
13. Lario D, Decker RB, Re-examination of the October 20, 1989 ESP event, Conf. Proc. of the ICRC 2001 07–15 August, Hamburg, p 3485
14. Mewaldt RA, Cummings AC, Cummings JR et al (1993) The return of the anomalous cosmic rays to 1 AU in 1992. Geophys Res Lett 20:2263
15. Dale CJ, Chen L, McNulty PJ, Marshall PW, Burke EA (1994) A comparison of Monte Carlo and analytic treatments of displacement damage in Si microvolumes. IEEE Trans Nucl Sci 41(6):1974–1983
16. Huhtinen M, Aarnio PA (1993) Pion induced displacement damage in silicon devices. Nucl Instrum Methods Phys Res Sect A 335(3):580–582
17. Akkerman A, Barak J, Chadwick MB et al (2001) Updated NIEL calculations for estimating the damage induced by particles and gamma rays in Si and GaAs. Radiat Phys Chem 62:301–331
18. Summers GP, Burke EA, Shapiro P, Messenger SR, Walters RJ (1993) Damage correlations in semiconductors exposed to gamma, electron and proton radiations. IEEE Trans Nucl Sci 40(6):1372–1379
19. Vasilescu A, Lindstroem G. Displacement Damage in Silicon, Online Compilation. http://sesam.desy.de/members/gunnar/Si-dfuncs.html. Accessed 15 July 2005
20. Walters RJ, Shaw GJ, Summers GP, Burke EA, Messenger SR (1992) Radiation effects in Ga0.47In0.53As devices. IEEE Trans Nucl Sci 39(6):2257–2264
21. Fodness BC, Marshall PW, Reed RA, Jordan TM, Pickel JC, Jun I, Xapsos MA, Burke EA, Ladbury R (2003) Monte Ccarlo treatment of displacement damage in bandgap engineered HgCdTe detectors. IEEE Conf. Proc., 7th European Conference on Radiation and its Effects on Components and Systems (RADECS), pp 479–485
22. Jun I, Xapsos MA, Messenger SR, Burke EA, Walters RJ, Summers GP, Jordan T (2003) Proton nonionizing energy loss (NIEL) for device applications. IEEE Trans Nucl Sci 50(6):1924–1928
23. Jun I, Kim W, Evans R (2009) Electron nonionizing energy loss for device applications. IEEE Trans Nucl Sci 56(6):3229–3235
24. Electronic Industries Association (EIA) (1996) Test procedures for the measurement of single-event effects in semiconductor devices from heavy ion irradiation. EIA/JEDEC Standard No. 57, Arlington, EIA, VA, p 49
25. JEDEC Solid State Technology Association (2006) Measurement and reporting of alpha particle and terrestrial cosmic ray-induced soft errors in semiconductor devices. JEDEC Standard No. 89A. JEDEC Solid State Technology Association 2001 Arlington, VA, pp 2201–3834

26. Bruguier G, Palau JM (1996) Single particle-induced latchup. IEEE Trans Nucl Sci 43:522
27. Pickel JC (1996) Single-event effects rate prediction. IEEE Trans Nucl Sci 43:483
28. Dodd PE (1996) Device simulation of charge collection and single event upset. IEEE Trans Nucl Sci 43:561
29. Sexton F (2003) Destructive single-event effects in semiconductor devices and ICs. IEEE Trans Nucl Sci 50:603–621
30. Schwank J, Ferlet-Cavrois V, Shaneyfelt M, Paillet P, Dodd P (2003) Radiation effects in SOI technologies. IEEE Trans Nucl Sci 50:522–538
31. Pease RL, Seiler J (2005) Evaluation of MIL-STD-883/test method 1019.6 for bipolar linear circuits. J Radiat Effects Res Eng. http://focus.ti.com/pdfs/hirel/space/HEART05-G1paper.pdf. Accessed 23 Nov 2016
32. American Society for Testing and Materials (ASTM) F1892 Standard guide for ionizing radiation (total dose) effects testing of semiconductor. West Conshohocken, PA : ASTM, 2006, Philadelphia, p 39
33. European Space Agency/Space Components Coordination (ESA/SCC) Basic specification n. 22900. Total dose steady-state irradiation test method. Issue 3, MAR 2007
34. Electronic Industries Association (1996) Test procedures for the measurement of single-event effects in semiconductor devices from heavy ion irradiation. EIA/JEDEC Standard, No. 57, Arlington
35. European Space Agency/Space Components Coordination (ESA/SCC) (1995) Basic specification n. 25100 Single event effects test method and guidelines, 1st edn. ESA
36. Virtanen A, Javanainen A, Kettunen H, Pirojenko A, Riihimäki I, Ranttila K. Radiation effects facility at JYFL. https://www.jyu.fi/fysiikka/en/research/accelerator/radef. Accessed 23 Nov 2016
37. Heavy ion irradiation facility (HIF). http://www.cyc.ucl.ac.be/HIF/HIF.php. Accessed 23 Nov 2016
38. Harboe-Sorensen R, Guerre FX, Roseng A (2005) Design, testing and calibration of a reference SEU monitor system. IEEE Conf. Proc. European Conference in radiation and its effects on components and systems. RADECS 2005, pp B3–1–B3–7
39. Harboe-Sorensen R, Poivey C, Guerre F-X, Roseng A, Lochon F, Berger G, Hajdas W, Virtanen A, Kettunen H, Duzellier S (2008) From the reference SEU monitor to the technology demonstration module on-board PROBA-II. IEEE Trans Nucl Sci 55:3082–3087
40. Iles PA (2001) Evolution of space solar cells. Sol Energy Mater Sol Cells 68:1–13
41. Bett AW, Dimroth F, Stollwerck G, Sulima OV (1999) III–V compounds for solar cell applications. Appl Phys A69:129–199
42. Priyanka Singh N, Ravindra M (2012) Temperature dependence of solar cell performance—an analysis. Sol Energy Mater Sol Cells 101:36–45
43. Green MA, Emery K, Hishikawa Y, Warta W, Dunlop ED (2012) Solar cell efficiency tables (version 39). Prog Photovolt Res Appl 20:12–20
44. Torchynska TV, Polupan GP (2002) III-V material solar cells for space application. Semiconduct Phys Quant Electron Optoelectron. 5(1):63–70
45. Li SS, Loo RY (1991) Deep-level defects and numerical simulation of radiation damage in GaAs solar cells. Solar Cells 31:349–377
46. de Angelis N, Bourgoin JC, Takamoto T, Khan A, Yamaguchi M (2001) Solar cell degradation by electron irradiation. Comparison between Si, GaAs and GaInP cells. Sol Energy Mater Sol Cells 66:495–500
47. Yamaguchi Masafumi (2001) Radiation-resistant solar cells for space use. Sol Energy Mater Sol Cells 68:31–53
48. Danilchenko B, Budnyk A, Shpinar L, Poplavskyy D, Zelensky SE, Barnham KWJ, Ekins-Daukes NJ (2008) 1 MeV electron irradiation influence on GaAs solar cell performance. Sol Energy Mater Sol Cells 92:1336–1340
49. Weinberg I (1991) Radiation damage in InP solar cells. Solar Cells 31:331–348
50. Sumita T, Imaizumi M, Matsuda S, Ohshima T, Ohi A, Itoh H (2003) Proton radiation analysis of multi-junction space solar cells. Nucl Instrum Methods Phys Res 206:448–451
51. Hacke P, Uesugi M, Matsuda S (1994) A study of the relationship between junction depth and GaAs solar cell performance under a 1 MeV electron fluence. Sol Energy Mater Sol Cells 35:113–119
52. Yamaguchi M (2001) Radiation-resistant solar cells for space use. Sol Energy Mater Sol Cells 31–53